D 1 D

GANIL

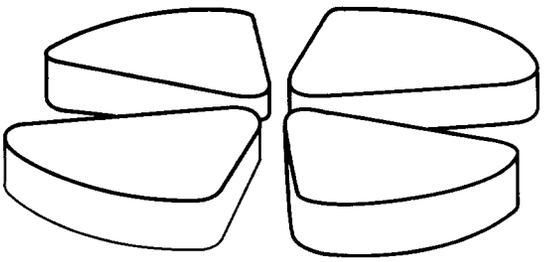

INTEGRAL MEASUREMENT OF BREAK-UP EXCITATION FUNCTION USING A MULTIPLE SILICON TELESCOPE

J.M. CORRE[1)], R. ANNE[1)], C. BORCEA[2)], V. BORREL[3)], F. CARSTOIU[2)], Z. DLOUHY[4)], A.S. FOMICHEV[5)], D. GUILLEMAUD-MUELLER[3)], M. LEWITOWICZ[1)], S.M. LUKYANOV[5)], A. KORDYASZ[6)], A.C. MUELLER[3)], F. NEGOITA[2)], YU.E. PENOINZHKEVICH[5)], F. POUGHEON[3)]. M.G. SAINT-LAURENT[1)], O. SORLIN[3)], N.K. SKOBELEV[5)]

[1)]GANIL, BP 5027, 14021 Caen Cedex, France
[2)]IAP, P.O.Box MG-6, 76900 Bucharest-Magurele, Romania
[3)]IPN, CNRS-IN2P3, 91406 Orsay Cedex, France
[4)]NPI, 25068 Rez, Rep. Czech
[5)]FLNR, JINR, 141980 Dubna, Moscow region, Russia
[6)]IFD, Warsaw Univ., Hoża 69, 00681 Warsaw, Poland

SW 9503

GANIL P 94 38

INTEGRAL MEASUREMENT OF BREAK-UP EXCITATION FUNCTION USING A MULTIPLE SILICON TELESCOPE

J.M. CORRE[1)], R. ANNE[1)], C. BORCEA[2)], V. BORREL[3)], F. CARSTOIU[2)], Z. DLOUHY[4)], A.S. FOMICHEV[5)], D. GUILLEMAUD-MUELLER[3)], M. LEWITOWICZ[1)], S.M. LUKYANOV[5)], A. KORDYASZ[6)], A.C. MUELLER[3)], F. NEGOITA[2)], YU.E. PENOINZHKEVICH[5)], F. POUGHEON[3)], M.G. SAINT-LAURENT[1)], O. SORLIN[3)], N.K. SKOBELEV[5)]

[1)]GANIL, BP 5027, 14021 Caen Cedex, France
[2)]IAP, P.O.Box MG-6, 76900 Bucharest-Magurele, Romania
[3)]IPN, CNRS-IN2P3, 91406 Orsay Cedex, France
[4)]NPI, 25068 Rez, Rep. Czech
[5)]FLNR, JINR, 141980 Dubna, Moscow region, Russia
[6)]IFD, Warsaw Univ., Hoża 69, 00681 Warsaw, Poland

Abstract

A simple method is proposed for measuring the inclusive break-up excitation function in which the experimental device, consisting of a set of succesive silicon detectors, serves the double purpose of decreasing the incident beam energy and of detecting and identifying the reaction products. Monte Carlo simulations revealed the merits and the limitations of the method. Finally, experimental data for tritons are treated in order to obtain relevant physical informations.

1. Introduction

The experimental method of measuring the excitation function of small angle break-up cross section proposed [1] in the present paper is most adequate for loosely bound projectiles and was initially devoted [2] to neutron halo nuclei like ^{11}Li and ^{11}Be, though later on it was tested on the more difficult case of tritons. The principle of the method and the procedures for determining the energy at the reaction moment are described in the next section; then, the complicating factors brought in by the finite resolution of the detectors and by straggling are also examined. The selection of interesting break-up events are presented in the following section for the test case of tritons. The merits and limitations of the mentioned procedures are tested in section 4 on simulated data before applying them to the real data in section 5, where the excitation function for the break-up of tritons (54 MeV incindent energy) is presented and briefly discussed. The tritons were obtained as a secondary beam at GANIL, using the doubly achromatic spectrometer LISE3 [3]. Some conclusions are formulated at the end.

2. The method

A somewhat special category of experiments in nuclear and particle physics is that in which the incident particles are stopped in a medium that plays the double role of target and detector. Trajectories of incident particles and reaction products are for example visualised in bubble chambers or streammer chambers or reconstructed in nuclear emulsions stacks. Also stacks of plastics or solid state nuclear track detectors can be used. Time projection chambers or Bragg ionisation chambers could serve the same purpose.

In the method presented here, for the double purpose of slowing down the incident beam and of recording and identifying the projectile fragments after the break-up, a multiple telescope of silicon detectors in which the incident beam is stopped is proposed to be used. This method is valid under some restrictive conditions, of which the most important are:

i) the energy needed to induce the projectile break-up is very small compared to the projectile energy;

ii) the projectile fragments continue to move after the reaction with an almost unchanged velocity vector with respect to that of the projectile (free break-up); consequently,

iii) only small reaction angles are considered or, equivalently, large impact parameters;

iv) the detecting material (silicon) serves also as target; in a first stage, only break-up reactions on Si are studied.

As the experiments on ^{11}Be dissociation showed, the above conditions are well satisfied for loosely bound projectile. Another experimental argument for the validity of our hypothesis is the narrow momentum distribution of the ^{9}Li resulting from the break-up of 28 MeV/u ^{11}Li on a Pb target [4]: the width is only $\sigma_{^9Li} = 18 \pm 4$ MeV and the corresponding angular

distribution is then characterized by $\sigma_\theta = 0.48 \pm 0.11°$.

In the cases examined in the present paper, the fragments complementary to the projectile-like one are neutrons that in most cases do not produce reactions in the silicon detectors. However, a recent experiment in which the break-up of ^{8}B into ^{7}Be and a proton was measured [1,5] showed the validity of the method also for this case and the obtained results will be published in a forthcoming paper.

Moreover, the situations in which a fragment of the projectile is captured by the target (break-up fusion) can be selected and subsequently eliminated, based on the induced recoil.

Figure 1 shows a Si detector in which a beam of e.g. 30 MeV/u ^{11}Li is stopped at a depth of about 6035 μm. Break-up reactions can take place all along this depth, the reaction energy varying from 30 MeV/u down to the threshold energy. If a break-up of ^{11}Li takes place on the very first layer of the detector, the resulting ^{9}Li will continue to move with the same velocity, having an energy of roughly 30 MeV/u (the two last neutrons are bound in ^{11}Li by only about 310 keV [6]) and it will be stopped after 4938 μm. The deeper inside the detector the break-up took place, the longer will be the total path from the front of the detector to the stop point of the projectile-like fragment (break-up product, in the given case ^{9}Li). This path —called stopping length— is a sum of two components: the first one in which the projectile energy is degraded from the incident energy to the reaction energy and the second one in which the break-up product is stoped. All these situations will give rise to trajectories whose total length will be comprised between the two limits defined above: from 4938 μm to 6053 μm.

Fig. 2a shows for this particular case of ^{11}Li the dependence of the stopping length on the depth inside the detector where the break-up occured, depth that can be directly related to energy at which the reaction took place. This is a univocal function that may be used to determine the energy as a function of stopping length (the stopping length can be easily determined if one knows the stop detector and the energy deposited in it). A similar dependence can be obtained for the total deposited energy as a function of the depth inside the detector where the break-up occured, as shown in fig. 2b. Of course, these curves refer to an idealised case. In a real case, angular and energy straggling, momentum distribution of the fragment and detector resolution will transform them into a "swarm" of events distributed with certain probability around initial curve, which means that the determination of projectile energy at the reaction moment will be affected by certain errors generated by the above probability distribution.

In fact, these curves reflect the conditions *i*)–*iii*). Similar curves can be plotted in the case when a thick target is used and the detectors are placed only in the stopping region. But, by emploing a target which is composed of detectors, one get more experimental control over the reaction events: better selection can be made and other methods of extracting reaction energy can be used. Therefore we will suppose that condition *iv*) is also fulfilled.

In the following E_r is the reaction energy and Q is the energy needed to break-up the projectile. The energy of the outgoing projectile-like fragment will be $q(E_r - Q)$, condition *ii*) imposing that q equals the ratio of the fragment and projectile masses. Then, if the incident energy is E_{inc}, the total energy deposited in the telescope will be:

$$E_{tot} = E_{inc} - E_r + q(E_r - Q)$$

wherefrom one can deduce the simple linear dependence

$$E_r = \frac{E_{inc} - E_{tot} - qQ}{1 - q} \tag{1}$$

The possibility of defining these methods comes, mainly, from the assumption that condition *ii*) is satisfied with enough accuracy; therefore they can be considered as model dependent. Another type of methods, that live the fragment velocity at the reaction moment as a free parameter, can be defined. Among them one could mention the following two prescriptions: a) a χ^2 method in which the reaction place x and the fragment energy after the reaction are searched such as to minimize the expression:

$$\chi^2 = \sum \left(\frac{E_i - E_i^c}{\delta_i} \right)^2$$

where E_i is the energy deposited in the i^{th} detector, E_i^c is the calculated energy deposited in this detector if the reaction took place at the depth x inside the telescope and δ_i is the error in determining the energy due to detector resolution and to straggling; b) a method that choses a reaction point and calculates, from given incident energy and stopping length, both the total energy E_{tot}^c and the q ratio. The quantity to be minimised is in this case:

$$test = |E_{tot}^c - E_{tot}^{exp}|.$$

As already mentioned, the factors complicating the above methods are: the finite detector resolution, the energy and angular straggling and the slight noncolinearities of the projectile and fragment directions. As for the other factors, their effect on the precision of various methods has been tested by extensive Monte Carlo simulations.

In order to determine the total length of the trajectory of a reaction event the detecting device has to be fragmented into many parts, especially the region where the stops are expected to occur. Besides, this fragmentation is a prerequisite for the correct identification of the reaction products by the energy loss–residual energy method. This imposes a limitation of the minimal reaction energy detected as the break-up product should pass across at least two detectors in order to be correctly identified. Obviously, the finer is this fragmentation, the more precise is the determination of the stopping length and the lower is the limit on the detected reaction energy. On the other side, a large number of detectors will increase the error of total deposited energy and will lower the angular acceptance of telescope. Therefore, an optimization should be performed.

3. Selection of reaction events – The test case of tritons

In this section a test experiment on tritons is used to illustrate the proposed method. The additional problems rised in this case – which is not a typical one in the field of applicability of the method – were enlightened.

The detectors of the telescope used in this test experiment are listed in table 1. The spacing between two succesive detectors was 10 mm and the front collimator accepted particles in a cercle with a diameter of 15 mm.

A beam of $^{36}Ar^{16+}$ with an energy of 27 MeV/u, delivered by the GANIL accelerating complex (in auxiliary mode), bombarded a target of 181.7 mg/cm^2 natural Ni. The reaction products were analysed by the doubly achromatic spectrometer LISE3 which was set to a rigidity of 1.824 Tm. At a current of 200 enA the rate of accumulated events was 70/sec. Besides the energy informations for each member of the telescope, position informations were taken from the first and fifth detectors and time of flight was measured between the signal taken from the second detector of the telescope, that served also as trigger for the aquisition system, and the cyclotron high frequency signal. The opening of the spectrometer slits permitted a variation of $\pm 5\%$ around the central energy of 54 MeV. However, for each individual event, the incident triton energy was determined from the time of flight information with an accuracy of 0.5%. From the species impinging on the telescope, the tritons were selected by setting appropriate gates on the two-dimensional energy loss – time of flight spectrum.

The two-dimensional spectra built from any two succesive detectors of the telescope were monitored during the run and rebuilt off line only for incident tritons. For these spectra, a veto condition was imposed, namely that no signal was recorded for a higher rank detector which means that the particle was stopped in that particular detector of the telescope. The events corresponding to escaped tritons or beam interaction in the considered pair of detectors which are not eliminated by this condition lie outside the region in which the stopped deuterons and tritons are placed. Then, using the Goulding procedure [7], the identification spectra were obtained. The FWHM of the two peaks, coresponding to stopped tritons and deuterons, was about 3.5 times smaller that the distance between their maxima permiting to set the selection gate for break-up events. The result of this analysis is shown in fig. 3 where, for 6 pairs of consecutive detectors, the energy loss in last detector vs. the Goulding indentification function value is plotted.

The identication is affected not only by detectors resolution and energy straggling, but also by the trajectory angle of detected particle. In the above representation, all the particules deviating from normal incidence are shifted to the right. For a 300 μm detector, a deuteron placed at equal distances from the deuteron and triton stripes coresponds to a radial angle of 31°. Comparing with angles marked in fig. 4, ones can see that this limitation act only for reactions at small energies. For larger reaction energies the angular limitation is practicaly determined by telescope geometry and beam distribution. As the reactions considered are direct ones with the characteristic forward focussing, the error in the evaluation of break-up cross section because of losses at large reaction angles should be small.

The tritons are a convenient case from point of view of the identification of break-up events, but the problem of determining the reaction energy is complicated by the fact that conditions *i*)–*iii*) are not rigorously satisfied. The binding energy of the neutron in the triton is $Q = 6.26$ MeV, not negligible as comparred to the incident energy; therefore deviations could appear from a colinear geometry and the velocity of produced deuterons could differ from that of tritons.

One should mention that in the present experiment events coming from channel d + anything are recorded as the neutron is either captured by the target nucleus (a stripping reaction) or, if not, as in the case of a free break-up, escapes detection due to its small interaction probability inside the telescope. In fact, due to the information given by each detector of the telescope, these two situations can be distinguished from one another. Indeed, for a stripping reaction, one would expect that the recoil energy of ^{29}Si formed after the capture of one neutron by the target will make the distribution of deposited energies in the telescope's detectors sensibly different from that of a free break-up taking place at the same energy, especially in the detector where the reaction occured. Only free-break-up events were considered in the subsequent analysis.

4. Test of the method by Monte Carlo simulations

In order to test the possibilities and limitations of the above mentioned procedures one has to apply them to cases for which one knows a priori the reaction place, the energy loss in each detector, the incident energy, the velocity change of the reaction products with respect to the projectile, etc. For this purpose, a program was elaborated that propagates through the detector a given particle – in our case a triton – accounting for energy loss, straggling and finite detector resolution. Different distributions for incident energy, incident angle and position can be generated. The distance between detectors and finite radius of detector active area can be varied in order to estimate the escaped particles due to angular straggling [9] and angular distribution of reaction products. In the course of this propagation the program has provisions for making that particle undergo a break-up, record the reaction place and continue propagate the reaction products to the end of their path. The projectile like fragment emission angle and energy may also be generated according to different prescriptions. In this way files of simulated events were generated for further use. A first positive test for the program was that the experimentally observed energy losses of the incident triton beam in each detector of the telescope and the corresponding dispersions caused by straggling effects and the finite detector resolution were correctly reproduced by the simulated events, as can be seen from Table 1 where the values are compared for the experimental and simulated events. Then, events were generated with a constant break-up cross section of 20 barns. The reaction angle was set to zero. The histogram of about 13000 reaction events thus created is well described by the calculated curve corresponding to the mentioned cross section (fig. 5). In the next step, the file with the energy losses in the telescope's detectors for each of the generated events has been processed with various methods in order to deduce the triton energy at the reaction moment. The histogram obtained by applying formula (1) is shown on the same figure. The difference between the generated reaction energy and the found one — the dispersion — is a measure of the method performance.

In fig. 6 the dispersion diagrams are shown, together with a gaussian fit for three methods. The first one makes use of formula (1). The second applies the procedure b)

described above. The last one use the dependence plotted in fig. 2a after modification for case of tritons. The results was practically unchanged when a gaussian angular distribution of reaction products with variance of 5° was used; simulating the mentioned experimental error of incident energy, the increase of the dispersion was about 15%. The FWHM of 1.0 MeV obtained for the case when one applies formula (1) reflect the overall intrinsic resolution of the detecting device (composed of individual resolution of each member of the telescope) and is not affected by the energy straggling or noncolinearities. The third method (fig. 6c) is affected by straggling and in a small measure by the resolution of the last touched detector.

Though the results of fig. 6 have a rather small dispersion they are obtained on the data generated with a fixed q ratio. One would like then to see what effect has a variation in this ratio on the deduced reaction energies. Variation was introduced in the event generation procedure as a gaussian with a $\sigma_q = 0.04$ and centered on $q = 2/3$. From (1) one sees immediately that

$$\delta E_r \simeq E_r \frac{\delta q}{1-q} \tag{3}$$

i.e. a linear dependence of error on reaction energy is expected. This effect can be seen in fig. 7 in which the number of events is plotted as a function of deduced reaction energy based on (1) for the file generated in the above mentioned conditions. The high energy edge of this plot is smeared but the general trend of the curve is preserved. In addition, the shape of the curve in fig. 7 after the maximal experimental energy (54 MeV in the given case) suplies information about the expected width of the q distribution.

The methods based on a minimisation procedure, which were supposed to give both E_r and q, turned out to give very flat minima and consequently unreliable results on the files of simulated data. The explanation for this surprising result is that, at the reaction moment,the two isotopes have almost the same velocity and consequently the same stopping power. This is not the case, for example, in the break-up of ^{8}B into ^{7}Be+p.

In fig. 8, E_{tot} is plotted vs. total path length The upper edge of the swarm coresponds to equal velocities, while all other cases are placed below. This provides an additional selection for the events of interest in the sense that all those events laying above the upper edge should be discarded as belonging to other reaction mechanism.

5. Experimental results

All the prescriptions of the previous section were applied to the set of experimental data for tritons. In fig. 9 is shown the histogram of reaction energy found according to formula (1). The high energy edge of this histogram overstrip the incident energy (54±1 MeV). The statistics after this limit is very weak , merely permitting an estimation for the upper limit of the width in q distribution: $\sigma_q \simeq 0.04$ around a central 2/3 value. The shape of the measured distribution would then be almost unafected below 45 MeV.

Fig. 9 presents, also, the dependence of the free break-up cross section on the reaction

energy. The cross section for the bin i of width ΔE_i in energy is given by the formula

$$\sigma_i = \frac{N_i}{M_i} \frac{A}{N_{Av} \rho \Delta x_i} \tag{2}$$

where N_i is the number of reactions appeared in the given energy bin, Δx_i is the thickness of the zone of the detector for which the degraded incident energies belong to the bin and M_i is the flux of projectiles incident on that zone. The energy binning used in this case was 5 MeV and the error bars come from the statistics on each bin. In this method every particle incident on the detector is recorded and traced down to its stop irrespective to the fact that a break-up event occured or not, therefore the total flux is monitored. The number of incident tritons selected using the time of flight–energy loss in second detector spectrum was 3.8×10^5 and more then 97% of them have been identificated as tritons when stop. Therefore the relative error made by taking the same M_i for all bins is smaller then 3%.

The fall off at small energies (below 18. MeV) is an artifact due to the necessity of having the deuteron passed through at least two detectors before coming at rest for identification purposes. Because the thickness of last detectors is about 300 μm and the energy needed for break-up is large, the identification can not be made for deuterons which stop after the first half of the ninth detector (fig.3). The smeared edge at these low energies is then due to the large straggling in trajectory length for the small energy.

6. Conclusions

A method was presented for measuring in one exposure the excitation function of the break-up cross section for loosely bound nuclei, especially for neutron halo/proton halo canditates. The method, as presented, is valid for silicon as target and also as detection device in a form of a multiple telescope. The principle has been tested on extensive Monte Carlo simulations and practical conclusions were drawn before applying the method to the case of tritons of 54 MeV incident energy. At the end, the excitation function for the free break-up of tritons is presented together with some remarks concerning the domain of realiability of the method.

References

[1] J.M. Corre, Thesis, Université de Caen, GANIL T 94 03
[2] C. Borcea et al., Proposal for an experiment at GANIL (E227), GANIL R 93 06, p. 82
[3] M. Lewitowicz and C. Borcea, Proposal for an experiment at GANIL (E168a)
[4] D. Sackett et al., Phys. Rev. C 48(1993) p. 118
[5] R. Anne and A.C. Mueller, Nucl. Instr. and Meth. B70(1992) p 276
[6] G. Audi, A.W. Wapstra, Nucl. Phys. A565(1993)
[7] F.S. Goulding et al., Nucl. Instr. and Meth. 31(1964)
[8] W. W. Wilcke et al., At. Data and Nucl. Data Tables 25(1980) p. 389
[9] J.D. Jackson, Classical Electrodinamics (Wiley, New York, 1975) p. 650

Figure captions

Fig. 1. Pathes of different events in the telescope: for simplicity we represent it as a continuous medium. The upper arrow schematize the range of ^{11}Li. The middle one corresponds to a break-up of ^{11}Li in the very first layer. The lower arrow is an intermediate case. Consequently, all ^{9}Li will stop within the hatched zone.

Fig. 2. Univocal functions relating the stopping depth (a) and the total energy deposited (b) to the reaction depth of ^{11}Li with 330 MeV incident energy.

Fig. 3. Goulding spectra allowing the selection of deuterons by appropiate windows (vertical bars).

Fig. 4. Telescope geometry is schematically presented here. Detectors have 20 mm diameter and are placed perpendiculary on the Oz axis (beam direction) one at each 10 mm. The fragment from a reaction in first detector (54 MeV reaction energy) can pass through 5 detectors before stopping. At the other extreme, at lowest indentificable reaction energy (18 MeV reaction energy), it must pass through 2 detectors. For 4 different reaction points, supposing a parallel beam, the larger reaction angle which still have efficency 1 is drawn. The grazing angles, calculated using ref. [8], are 2.8° at 54 MeV and 8.7° at 18 MeV.

Fig. 5. We show here three steps of our analysis with Monte Carlo simulation. The thick line is obtained inversing formula (2) and setting a constant cross section of 20 b. The dots are the results of simulation; the distance between them and the full curve is due to statistical fluctuations. Finally, the histogram of reaction energies calculated with formula (1) is plotted.

Fig. 6. Comparison between the dispersions given, in analysis of simulated events, by three methods: (a) – formula (1), (b) – method b) (see text), (c) – the method using the dependence of reaction energy on stopping length.

Fig. 7. Same as the fig. 3 but with $\sigma_q = 0.04$. Only the high edge of the plot is modified.

Fig. 8. Two-dimensional scatter-plot of simulated events giving the accessible area for free break-up events when $\sigma_q = 0.04$.

Fig. 9. Experimental break-up excitation function (dots and left scale) and corresponding histogram of reaction energies (dashed line and right scale). Reaction energy was calculated applying formula (1) on the experimental events identificated as deutrons in fig. 3 (425 events) and selected as free break-up (353 events) using the spectrum plotted in fig. 8.

Fig. 1.

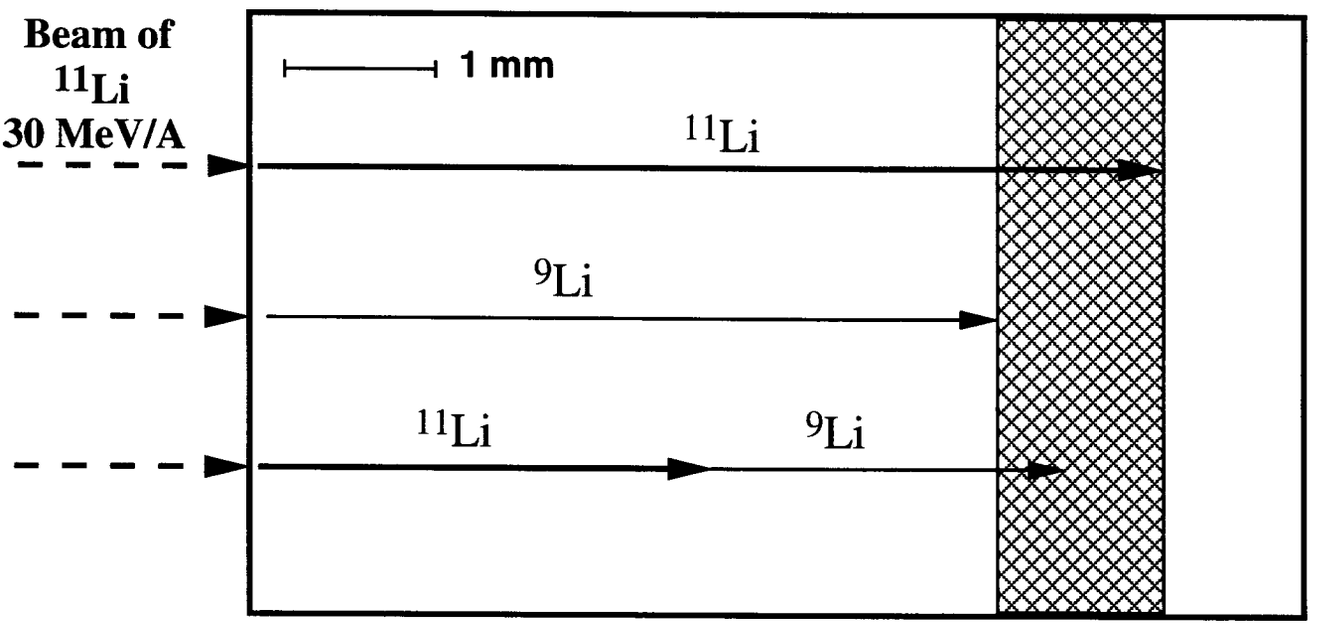

Fig. 2.

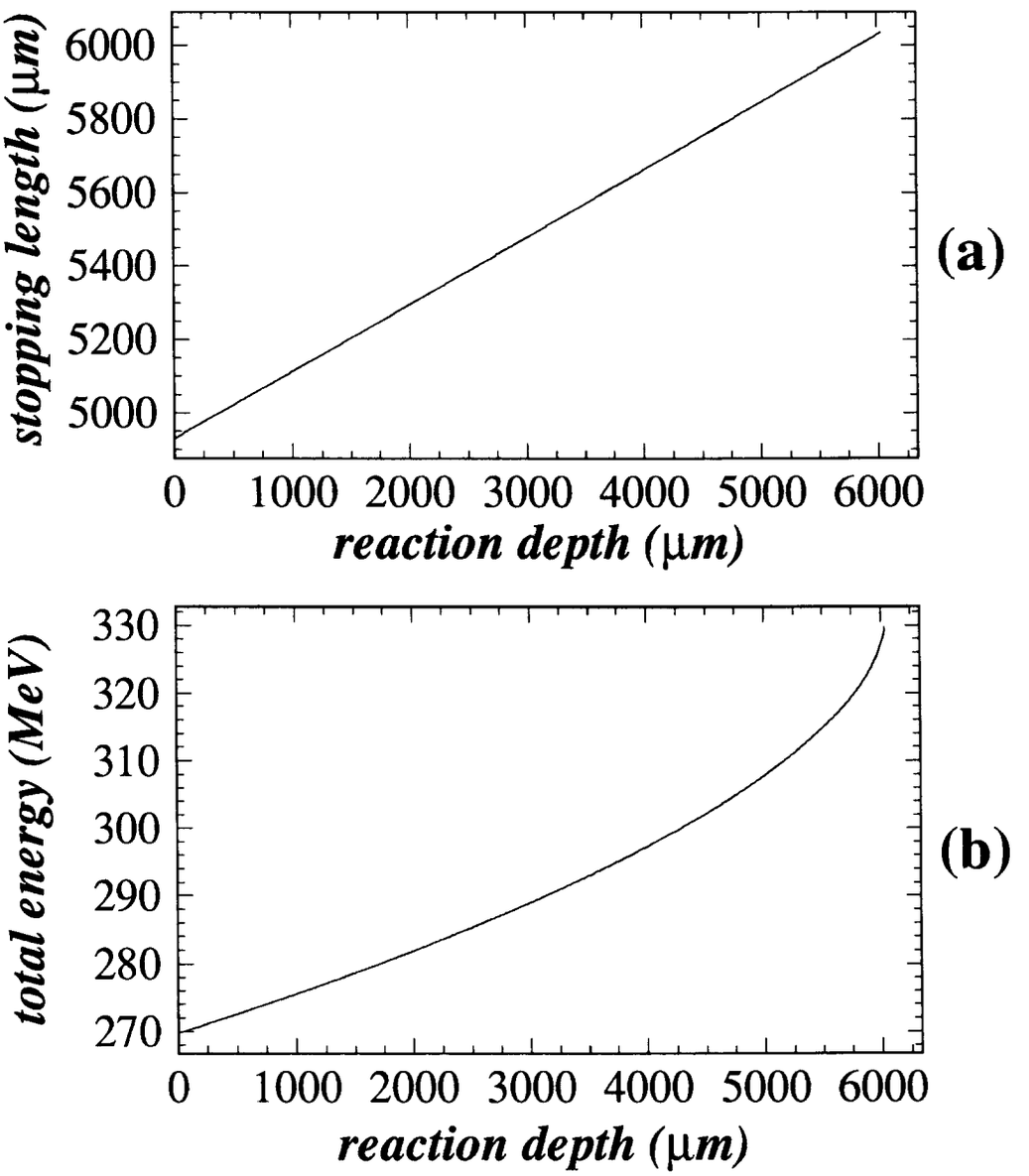
stopping length (μm)
6000
5800
5600
5400
5200
5000
0
1000
2000
3000
4000
5000
6000
reaction depth (μm)
(a)
total energy (MeV)
330
320
310
300
290
280
270
0
1000
2000
3000
4000
5000
6000
reaction depth (μm)
(b)

Fig. 3.

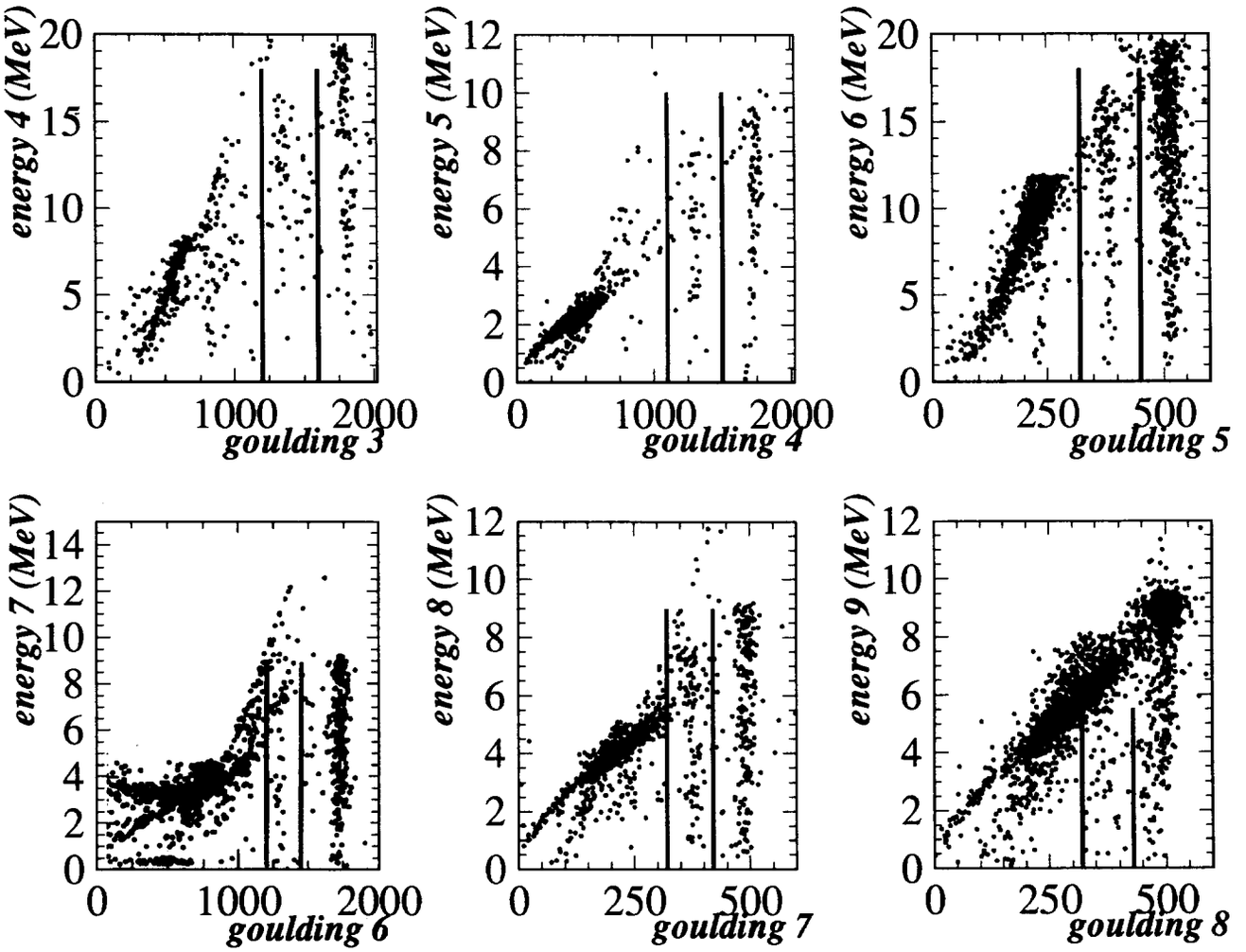
energy 4 (MeV)
goulding 3
energy 5 (MeV)
goulding 4
energy 6 (MeV)
goulding 5
energy 7 (MeV)
goulding 6
energy 8 (MeV)
goulding 7
energy 9 (MeV)
goulding 8

Fig. 4.

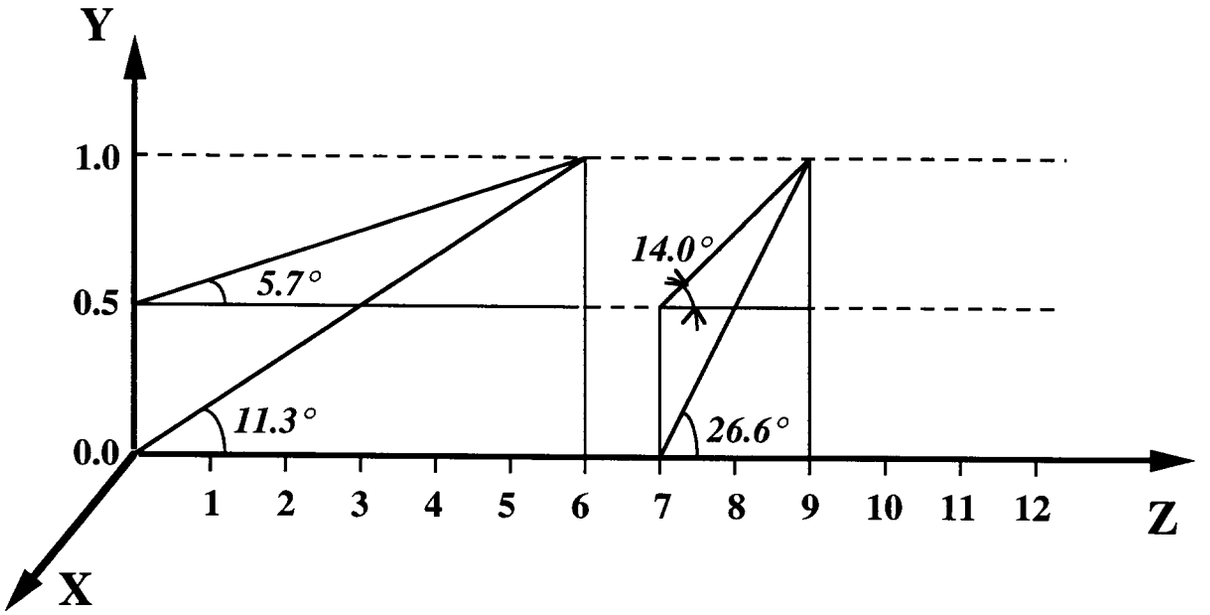

Fig. 5.

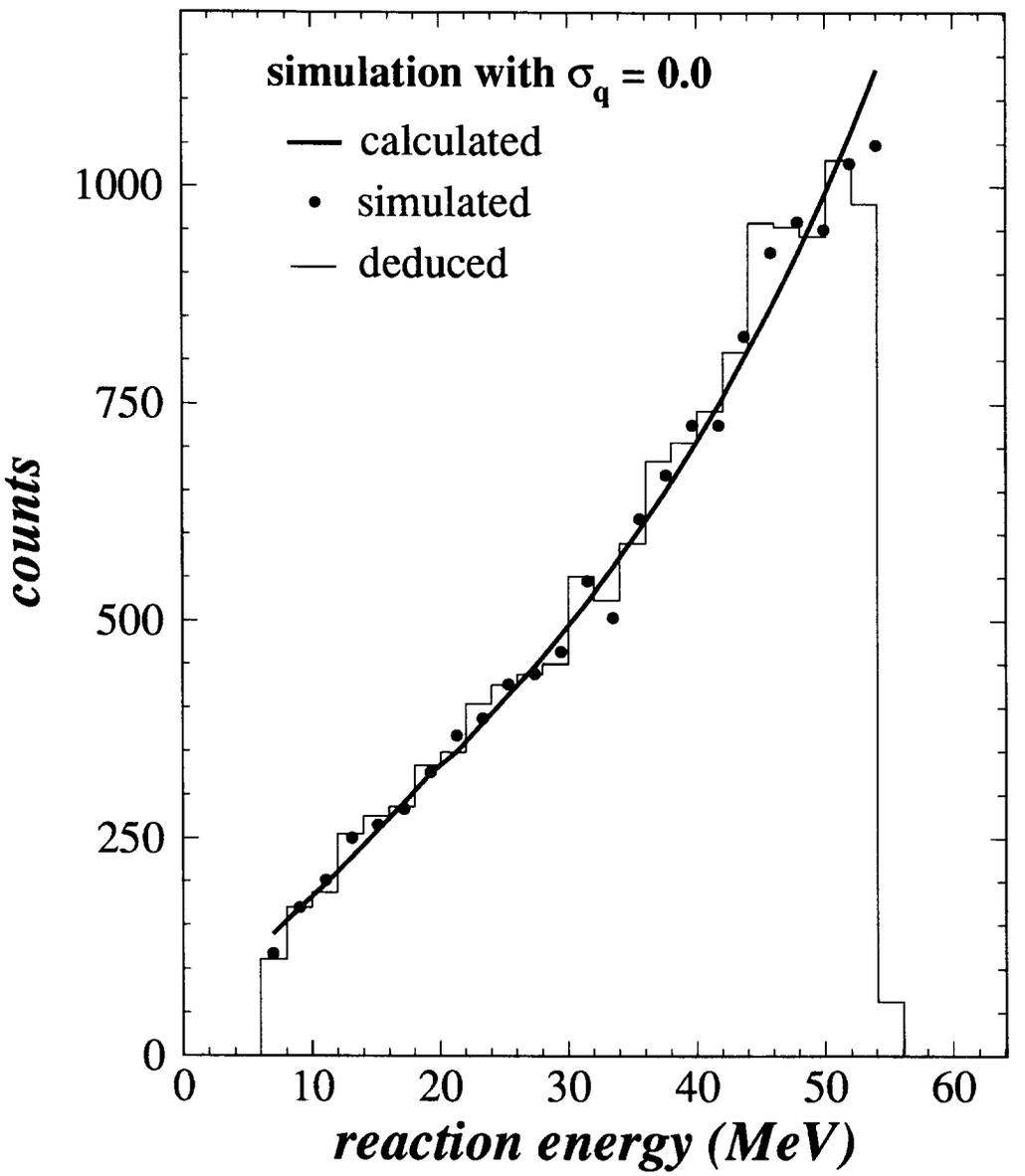
simulation with σ_q = 0.0
calculated
simulated
deduced
counts
reaction energy (MeV)
0
250
500
750
1000
0
10
20
30
40
50
60

Fig. 6.

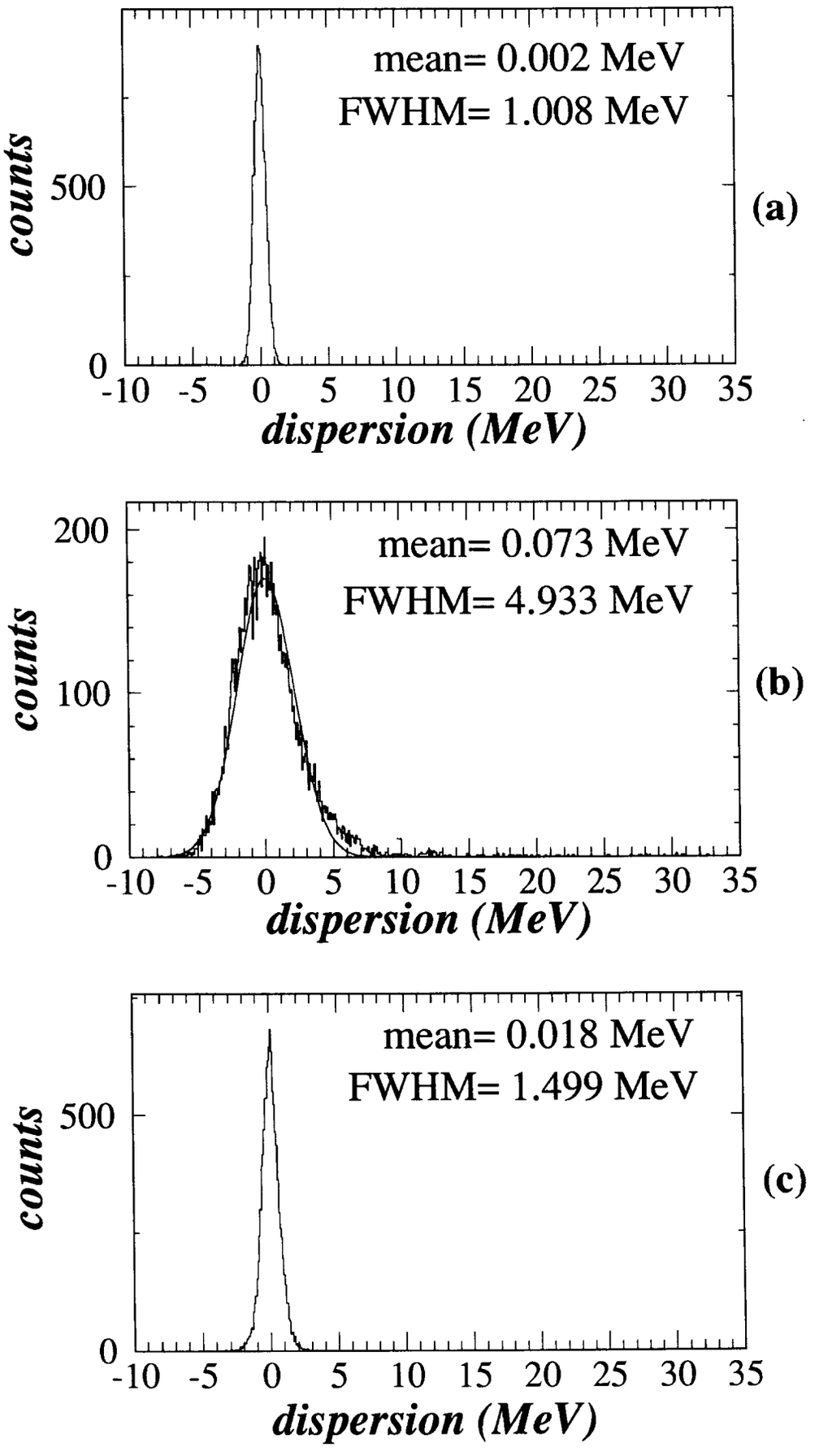
mean= 0.002 MeV
FWHM= 1.008 MeV
counts
500
0
-10 -5 0 5 10 15 20 25 30 35
dispersion (MeV)
(a)
mean= 0.073 MeV
FWHM= 4.933 MeV
200
100
0
(b)
mean= 0.018 MeV
FWHM= 1.499 MeV
(c)

Fig. 7.

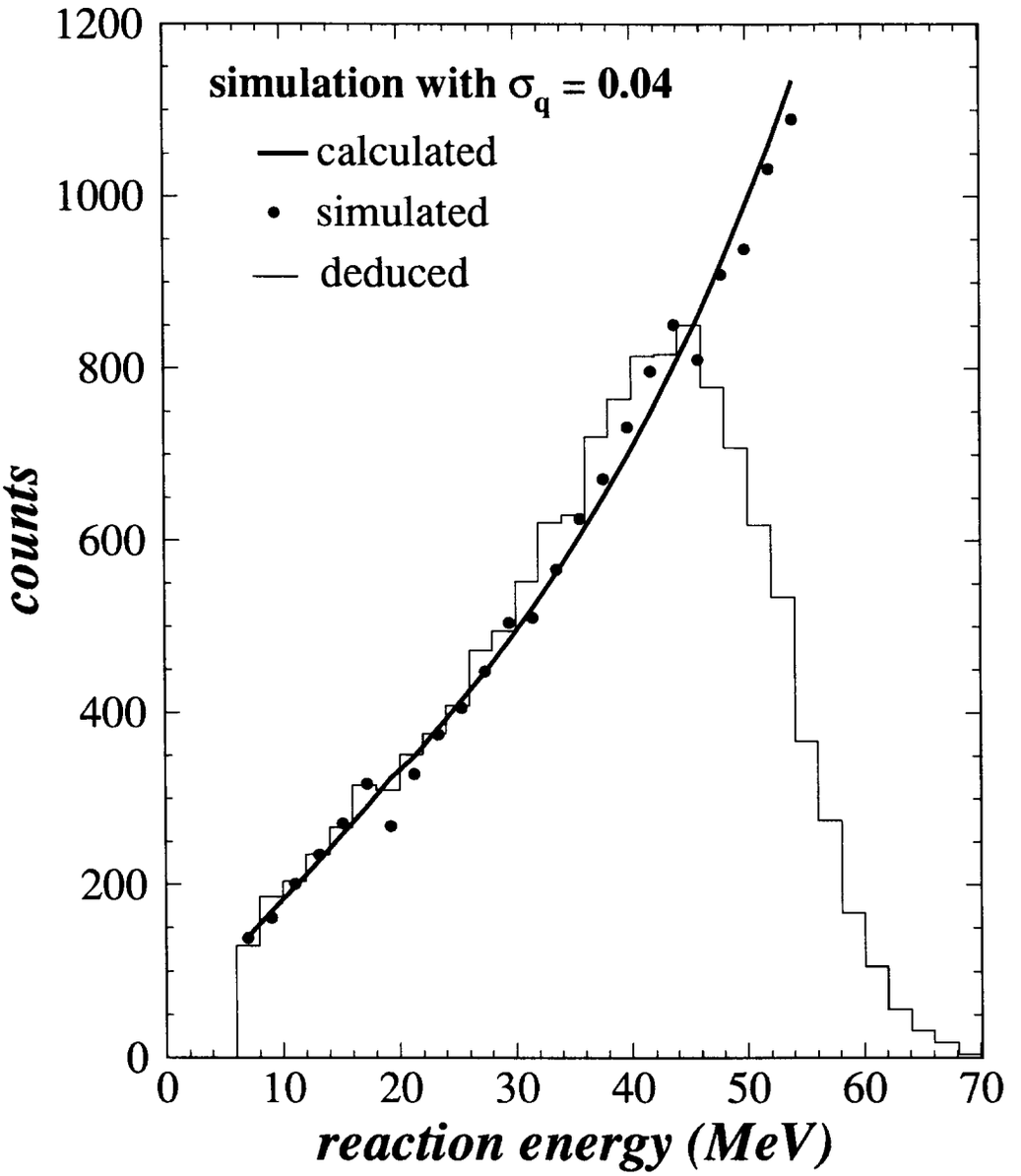
simulation with σ_q = 0.04
calculated
simulated
deduced
counts
reaction energy (MeV)
0
200
400
600
800
1000
1200
0
10
20
30
40
50
60
70

Fig. 8.

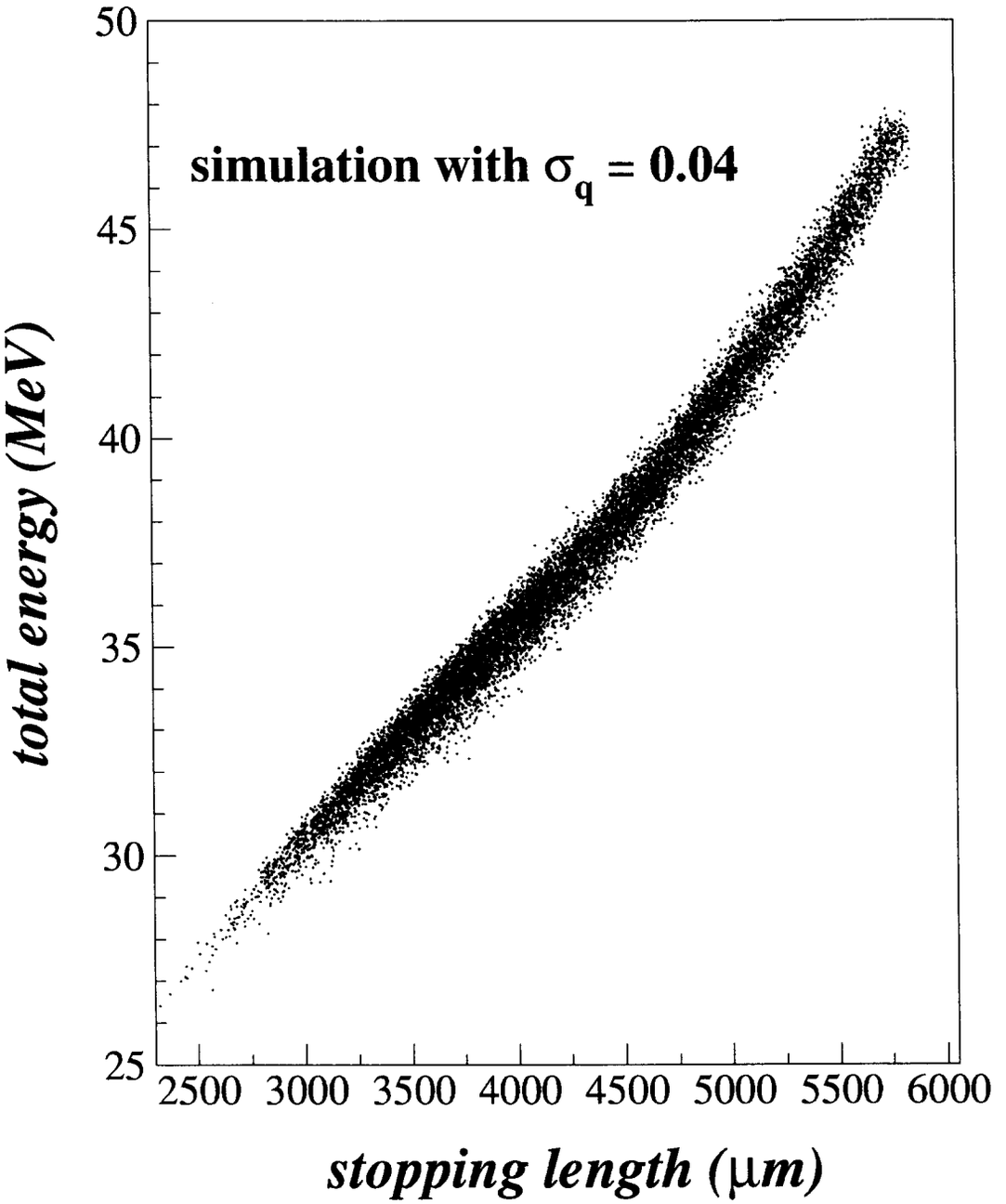
simulation with σ_q = 0.04
50
45
40
35
30
25
2500
3000
3500
4000
4500
5000
5500
6000
total energy (MeV)
stopping length (μm)

Fig. 9.

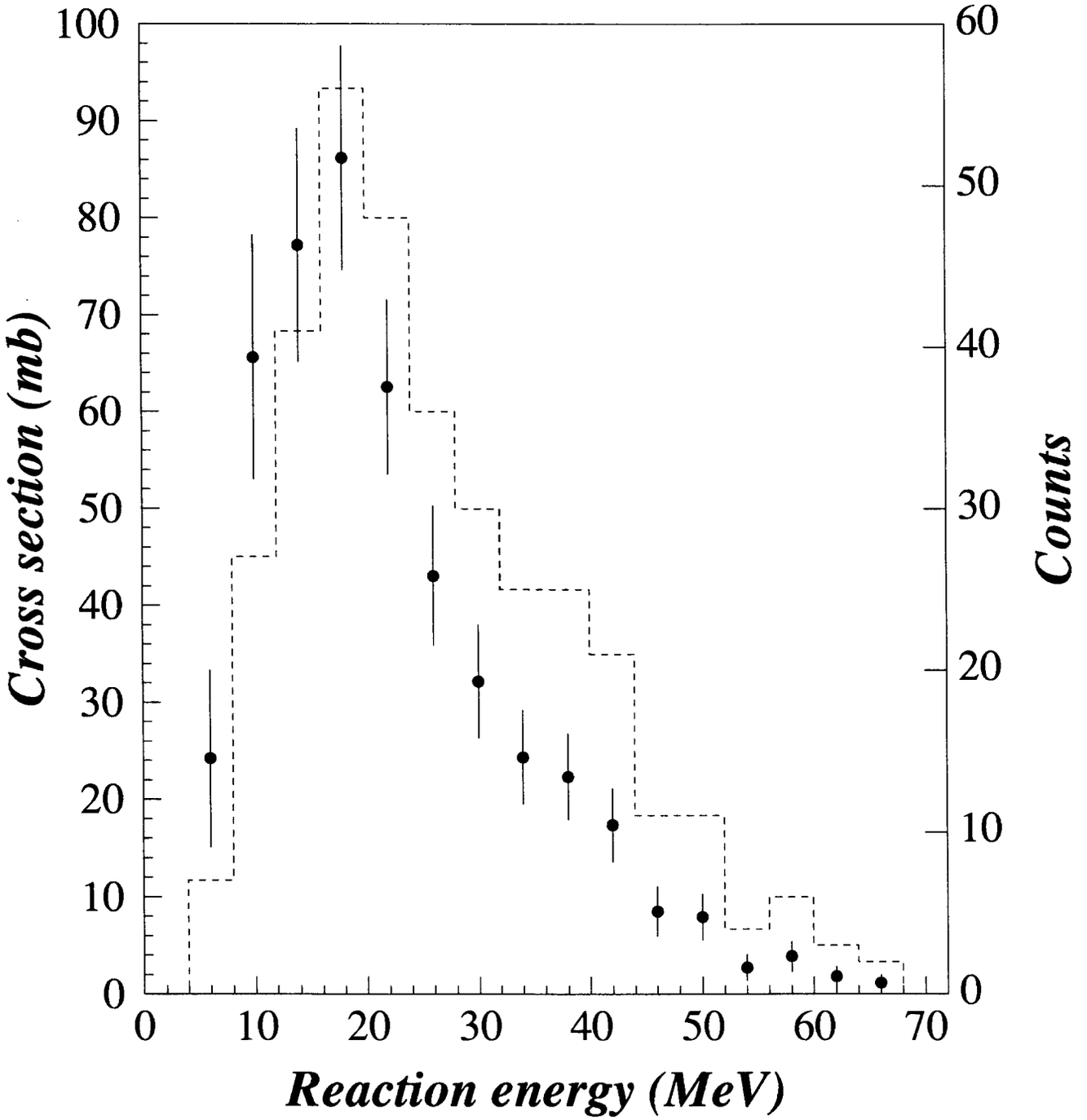
Cross section (mb)
Counts
Reaction energy (MeV)
0
10
20
30
40
50
60
70
80
90
100

Table 1.
In order to compare the experimental (exp.) and simulated (M.C.) energy losses in the telescope, a quasimonoenergetic beam of tritons (54. MeV) was considered and a gaussian function was fitted for each energy loss spectrum. A resolution of 140KeV for all detectors was used in the simulation, but the main contribution to obtained widths is given by energy straggling. Also due to the straggling ($FWHM_{range}$=110μm), the tritons were stopped in both 10^{th} and 11^{th} detectors.

detector	thickness	mean (MeV)		FWHM (MeV)	
	(μm)	exp.	M.C.	exp.	M.C.
1	450	2.20	2.36	0.378	0.261
2	1000	5.59	5.56	0.374	0.376
3	1000	6.31	6.15	0.411	0.369
4	1000	7.03	7.03	0.407	0.383
5	303	2.27	2.38	0.261	0.228
6	1017	9.21	9.19	0.590	0.449
7	294	3.22	3.23	0.301	0.284
8	311	3.80	4.06	0.437	0.378
9	298	-	-	-	-
10	303	-	-	-	-
11	301	-	-	-	-